Impedance Analysis of Automotive High Voltage Networks for EMC Measurements

Dipl.-Ing. M. Reuter[1*], Prof. Dr.-Ing. S. Tenbohlen[1], Dr.-Ing. W. Köhler[1], Dipl.-Ing. A. Ludwig[2]

[1] Institute of Power Transmission and High Voltage Technology (IEH), University of Stuttgart, Germany,

[2] Research & Technology, Daimler AG, Boeblingen, Germany

[*] Martin.Reuter@ieh.uni-stuttgart.de

Abstract — **The increasing demand of electric power in electric vehicles cannot be supplied by conventional automotive power networks. Therefore novel power bus systems, capable to deliver the required power are under development. These bus systems have higher operating voltages, which result in lower current amplitudes for power transmission. As power efficiency is one of the main factors determining the range of an electric car with a given battery capacity, fast slew rates of the power semiconductors are preferred. But with increasing slew rates also emitted radio frequency (RF) disturbances increase. To reduce electromagnetic interferences (EMI) of power electronics a complete shielding of the power bus system is necessary. Thus the network configuration is changed from unshielded single core multi wire harnesses into coaxial conductor layouts, and therefore also the impedance characteristics of the entire network are changed. Electromagnetic compatibility (EMC) of automotive components is measured according to CISPR 25, substituting the vehicle environment with line impedance stabilization networks (LISN). Recent research shows that LISNs, developed for low voltage networks, are not ideal to measure conducted emissions of high voltage (HV) components because of changed characteristic impedances and additional shielding.**

This paper deals with a method of determining the high-frequency impedances of automotive HV power networks. A Vector Network Analyzer (VNA) is used to measure Scattering parameters of different HV power cables and an automotive Li-Ion accumulator battery. Matrix conversions allow calculating an impedance network, which is able to represent an automotive HV networks.

Index Terms — *EMC, Automotive HV Networks, Characteristic impedance, HV LISN, RF charactersistics of Li-Ion battery*

I. INTRODUCTION

The electrification of the automotive power train requires a novel electrical power bus system. Recent automotive low voltage (LV) networks (12 V) are not able to meet power demands of electric driving engines because of high currents required for power transmission. Automotive high voltage (HV) power networks, with voltage levels of typically 120 - 380 V, reduce needed currents to values, which can be handled more efficiently.

One major task in developing electric cars is to control their electromagnetic interferences (EMI). Maximum efficiency of power electronics requires fast slew rates of switching semiconductor devices. But fast slew rates result in bus disturbances consisting of radio frequency (RF) spectral components with high amplitudes.

These RF disturbances may propagate along HV power lines and are able to interfere with other electronic devices.

Filters are a very strong element for suppression of conducted electromagnetic emissions (EME), but effective filter design requires knowledge about characteristic impedances of devices under test (DUT) and connected HV networks [1].

To ensure system's EMI performance, CISPR 25 defines an artificial network (AN/LISN), which represents a normalized automotive LV network with a standardized input impedance [2]. Every automotive component is tested regarding its EMI performance with this network. Devices connecting LV and HV network, e.g. DC/DC couplers, have to be terminated at their HV side connectors comparable to their vehicle environment. Basically, the LV LISNs can be used as HV termination, even shielding can be taken into consideration. However, this paper shows that wave impedances of HV cables differ substantially of the LV network characteristic impedance.

HV network impedance knowledge therefore is necessary for an effective HV filter design and to enable component EMI measurements with a realistic line impedance representing a vehicle environment.

This paper presents a method to characterize automotive HV network impedances for simulation of an automotive HV environment. The simulation of a real vehicle environment is a basic requirement for comparable EMC measurements that allows to estimate their later performance when mounted in an electric vehicle.

II. LISNS FOR CONDUCTED EMI TESTING

In 1983 a method was developed to measure conducted emissions of automotive components [3]. A Line Impedance Stabilization Network (LISN) was presented that provided mainly three functions:

1. Defined input impedance emulating a vehicle LV power network
2. Supply DUT with DC power
3. Impedance matching network to measurement system and decoupling of ambient distortions

This LISN was developed by impedance measurements at automotive LV networks having two conductors, battery plus (BP) and battery minus (BM), which usually is grounded to autobody on its LV bus far end. Fig. 1 shows a common two LISN EMI test setup.

Trying to use this LISN for HV component measurements two essential barriers occur: HV shielding and changed network input impedance.
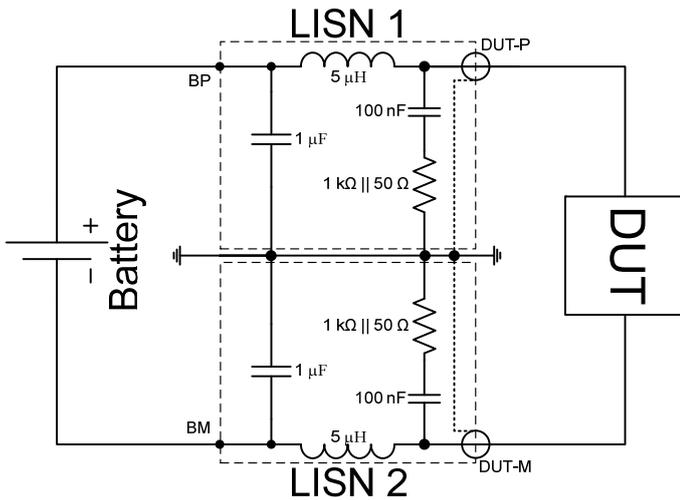
Figure 1.   Electric circuit of a two LISN setup for LV automotive component conducted EMI testing.

In order to reduce emitted RF radiation of HV power electronics a complete shielding of the HV system is used. As in 1983 there was no need for any shielding of electrical power systems, the AN is not intended to emulate a shielded system. For security reasons HV systems are assembled floating, thus BM is not grounded. This directly leads to a three conductor system, whereas the emulated system of the CISPR 25 is an unshielded two conductor system.

By inserting two LISNs into a shielded box, connecting BP to one AN, BM to the second and Ground to the HV cable shields the changed conductor layout can be taken into consideration (see fig. 1). This leads to an input impedance of 100 Ω between BM and BP and of 50 Ω between each conductor to ground. As the characteristic wave impedances of the coaxial HV cables is significantly lower than 50 Ω there is a mismatching of these transmission lines and standing waves and resonances can occur; hence it is not possible to evaluate the EMI performance of a HV component as in its vehicle environment.

Recent electric driven cars usually have their electric engine located in the front area and the accumulator battery in the back, connected by HV cables with the length of 3-4 m. Emitted RF power is mainly generated by fast switching power electronics, which are placed near the electric engine in the front. Conducted EMI can be coupled in cable wires (LV and HV), and is able to interfere with other connected systems. But these cable wires also act as antennas and emitted RF radiation may also disturb galvanically isolated systems such as sensitive radio antenna preamplifiers. In the investigated frequency range the radiated RF power of long cable harnesses is much higher than radiated EMI of the device itself (mainly housing). Thus for EMI performance of the complete system its conducted RF power on these long cables is essential [1].

Conducted emissions on automotive LV buses can be measured using ANs according to CISPR 25. If these ANs are used to emulate HV networks, disturbing RF sources of HV components are loaded with impedances of LV networks, which are different to the load impedances of the automotive HV environment. The measurement error cannot be corrected, as it is impossible to determine source impedances of RF sources (switching power semiconductors). A network

emulating automotive HV networks as close as possible, would load HV components as in their vehicle environment and enables correct EMI performance measurements. This network should simulate 3-4 m of HV cable with attached accumulator battery, as every HV component is connected to this minimum network. More complex networks can be partitioned and reduced to such a minimum HV network.

III.   HV CABLE MEASUREMENTS

For investigation of their RF behavior, six different automotive HV cables have been examined with a Vector Network Analyzer (VNA). That instrument is used to measure Scattering- or S-parameters of electronic circuits and networks.

The main high frequency attribute of a cable is its characteristic or wave impedance, which is determined by its line inductivity and capacity to ground. This chapter shows how to calculate these values of measured S-Parameters.

A.   Devices under Test – HV cables

Table 1 introduces six different HV cables, which have been investigated. All cables, except cable 1, are of the same manufacturer. Cable 6 is not a coaxial type shielded wire (as the others are); this cable has a common shield for both conductors.

TABLE I.   INVESTIGATED HV CABLES AND THEIR ASSEMBLY

	Cross Section	Type of shielding
Cable 1	25 mm²	Single conductor with shield and screening foil
Cable 2	25 mm²	Single conductor with shield and screening foil
Cable 3	25 mm²	Single conductor with meshed shielding, no foil
Cable 4	35 mm²	Single conductor with shield and screening foil
Cable 5	50 mm²	Single conductor with shield and screening foil
Cable 6	2x6 mm²	Two conductors with common shield and screening foil

All cables have a length of ℓ = 1 m, connected via low impedance cable glands to brass adapter boxes for N-Type RF connections to the measurement system, as shown in fig. 2. To obtain maximum analogy to vehicle situation two cables of the same type are arranged parallel to each other in a mutual distance of d = 4.25 cm. As cable 6 has a common shielding of both lines, these wires are spaced by the assembly of their isolation material inside the cable, having a minimum thickness of 0.28 mm. The cables are situated in a height of h = 5 cm above a conductive, grounded plane as shown in fig. 3.
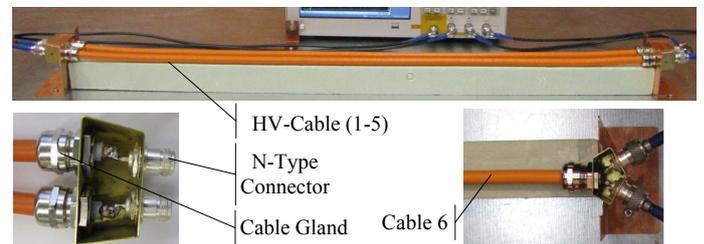
Figure 2.   HV cable assembly with brass adapter boxes and low impedances cable glands.

B. Measurement Setup

The S-parameters of the HV cables are measured with an Agilent ENA E5070B network analyzer in a frequency range of f = 300 kHz – 200 MHz. A mechanical calibration kit is used.
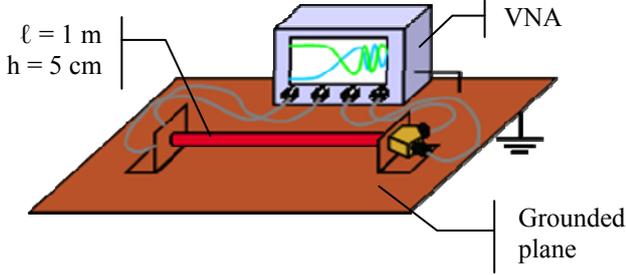
Figure 3.   Measurement setup of HV cable 6 with VNA to determine RF behavior (S-parameters).

C. Characterization Methodology

S-parameters are the quotient of reflected or transmitted wave to incident wave amplitudes. They are usually measured in a 50 Ω system and can easily be converted to Z-, Y-, H- and T-parameters. But they do not lead directly to the characteristic attributes of the measured transmission line. Characteristic cable values like wave impedances, line inductivities, ground capacitances or dielectric constants need to be calculated in further steps, which are presented in following chapters. [5]

D. Calculation of Line Impedances

For an impedance characterization these S-parameters need to be connected to a given electric network. An electric equivalent circuit (EEC) of these cables can be found in fig. 4. The simplest EEC of a transmission line is a T-network [1]. As the DUT consists of two parallel coaxial conductors a horizontally mirrored T-network is needed, as shown in fig. 4.
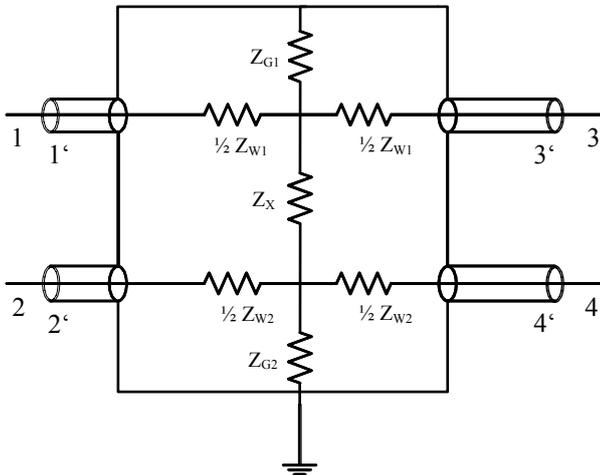
Figure 4.   Electric equivalent circuit of HV cable, with conductor 1 between ports 1-3, conductor 2 between ports 2-4 and cross coupling impedance Z_X.

Calculating the Z-parameters of this 1st order, horizontally mirrored T-network leads to an equation system of five different equations having five unknowns (Z_{W1}, Z_{W2}, Z_X, Z_{G1}, and Z_{G2}). Inverting this equation system to the unknowns delivers

$$Z_{W1} = 2\,Z_{11} - 2\,Z_{31}$$

$$Z_{W2} = 2\,Z_{22} - 2\,Z_{42}$$

$$Z_X = \frac{Z_{31} - Z_{42}}{Z_{12}} - Z_{12}$$

$$Z_{G1} = \frac{Z_{12}^2 - Z_{31} \cdot Z_{42}}{Z_{12} - Z_{42}} \, .$$

$$Z_{G2} = \frac{Z_{12}^2 - Z_{31} \cdot Z_{42}}{Z_{12} - Z_{31}}$$

The measured S-parameters are transformed into Z-parameters and inserted in this equation system. An example for cable 1 is shown in fig. 5.
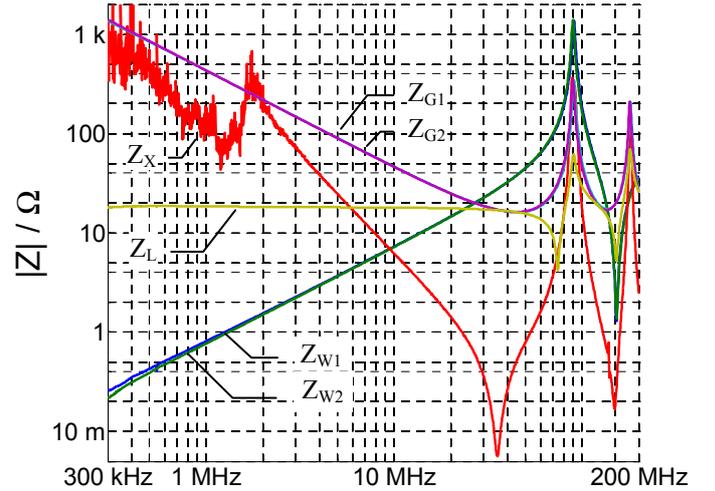
Figure 5.   Values of HV cable 1 equivalent circuit passive resistances vs. frequency.

Fig. 5 shows that the through resistances Z_{W1} and Z_{W2} start at a relatively small value (~150 mΩ), increase linearly until approximately 50 MHz and begin to oscillate above that. The resistances of inner conductor to grounded shielding (Z_{G1} & Z_{G2}) decrease linearly from 1 kΩ with increasing frequency and also oscillate above 50 MHz. Fig. 5 also shows that both conductors act very similarly, as the curves of Z_{W1}/Z_{W2} and Z_{G1}/Z_{G2} are nearly without distinction; they are even equal for most of the investigated frequency range. The cross coupling resistance Z_X does not show a clear frequency dependant behavior, but also oscillates in RF range. There are two clearly distinguishable frequency ranges of the line impedances: From 300 kHz to approximately 30 MHz the cable impedances have characteristic frequency dependencies, whereas above an oscillating behavior occurs. This results due to the quotient of wavelength to cable length: At $\lambda(f)/\ell < 6$ the cable is in quasi-stationary mode, acting like a network of concentrated elements, and at $\lambda(f)/\ell \geqslant 6$ its transmission line characteristics overbalance and lead to this oscillating behavior [1].

E. Impedance Interpretation

The first resonance of the investigated HV cable 6 is calculated as first maximum of Z_{W1} (see fig. 5). The resonance occurs at $\ell = \lambda/2 = 1$ m. In this example $f_R = 84.4$ MHz, meaning that at this frequency the wavelength is $\lambda_R(f) = 2$ m. In

air an electromagnetic wave at $f = 84.4$ MHz has a wavelength of $\lambda = c_0/f = 3.55$ m. This shortening effect can be traced to the isolation material dielectric constant

$$\varepsilon_r = \left(\frac{c_0}{2\ell \cdot f_{R1}}\right)^2.$$

In the quasi stationary region of the frequency range, line and ground impedances show linear frequency dependencies. In this range line impedances are inductive and ground impedances are capacitive. The line inductivity is determined by

$$L_S = \frac{Z_{W1}}{2\pi f},$$

and the capacity to ground is calculated via

$$C_G = \frac{1}{2\pi f \cdot Z_{G1}}.$$

There are two different ways of calculating wave or characteristic impedance of a transmission line [4]:

$$Z_L = \sqrt{Z_{11}^2 - Z_{31}^2}$$

$$Z_L^* = \sqrt{\frac{L_{Serial}}{C_{Ground}}}$$

Both formulas lead to an equal result, and are used to verify calculations. As both ways of determining the wave impedance do not have anything in common but the raw data, a similar result indicates correct calculation methodology. Fig. 6 shows an example for a graphical impedance analysis of cable 1.
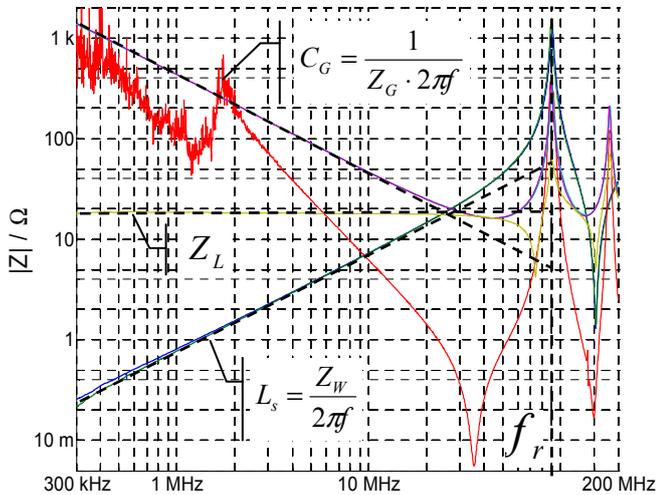
Figure 6 Graphical evaluations of cable 1 characteristic attributes C_G, L_S, Z_W and f_R.

F. Measurement Results

Table 2 lists the measured HV cable characteristics. It shows, that coaxial type shielded HV cables have a wave impedance in a range of $6.2 - 18.3\ \Omega$, with direct dependency to their geometrical properties.

TABLE II. CALCULATED TRANSMISSION LINE ATTRIBUTES OF AUTOMOTIVE HV CABLES

DUT	Cross Section / mm²	Z_L / Ω	L_S in nH/m	C_G in pF/m	$\sqrt{\frac{L_S}{C_G}}$ / Ω	f_R / MHz	ε_r
Cable 1	25	18.3	123	363	18.4	89.8	2.7819
Cable 2	25	11	70	575	11.0	84.4	3.1521
Cable 3	25	11	68	553	11.1	85.8	3.0465
Cable 4	35	14.7	102	466	14.8	84.8	3.1252
Cable 5	50	6.2	43	1102	6.3	85.8	3.0465
Cable 6	2 x 6	19.5	120	268	21.1	88.0	2.8977

Compared to usually estimated values of automotive low voltage cables ($L_S \approx 1\ \mu H/m$, $C_G \approx 100$ pF/m) these measurements show around 10 - 20 times smaller line inductivities and 3 - 10 times higher ground capacity values. This leads to considerably smaller wave impedances of HV networks.

Due to their high line inductivity LV networks have relatively high line impedance in the frequency region of interest for EMC issues. Additionally the transmission line character of HV cables is dominant above 10 MHz, where termination is defining its input impedance. Thus termination of HV cables becomes more important and has to be taken into account, because it is determining the input impedance of a HV network in combination with cable characteristic impedance.

IV. BATTERY MEASUREMENTS

As termination becomes important for the input impedance of a HV network, the HV batteries also need to be characterized. For all fast switching power electronics the termination of extended HV cables is an HV accumulator battery. The impedance of this battery is transformed by the transmission lines into a different input impedance of the entire network.

In this paper an automotive Li-Ion battery model is presented, having an operating voltage of $V_{op} = 128.9\ V_{DC}$ at 58.3 % state of charge (SOC). For the measurements a Rohde & Schwarz ZVR network analyzer is used. Fig. 7 shows the measurement setup, consisting of battery, battery controller, DC blocking device and VNA.
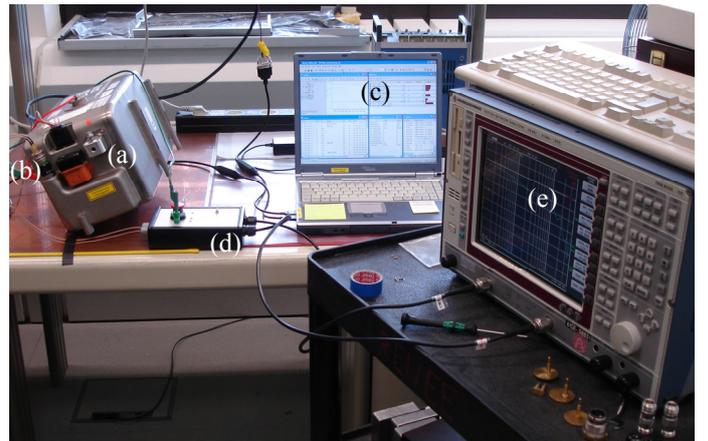
Figure 7 Measurement setup with Li-Ion battery (a), ECTA-SMB adapter (b), battery controller (c), DC blocking device (d) and VNA (e).

A. DC blocking Device

As the used network analyzer does not tolerate higher input voltages than $10\,V_{DC}$, high-pass filtering is required. To reject DC voltage a series capacitor of size $C_{Series} = 100\,nF$ is used. Combined with the input impedance of the VNA $R_{in,VNA} = 50\,\Omega$ this capacitor forms an RC high-pass filter, having a 3dB cut-off frequency of 31 kHz. The upper cut-off frequency of this filter is determined by the equivalent series inductance (ESL) of the used SMD capacitor components, and measurements verified it to be around 500 MHz. This band pass filtering behavior of the measurement adapter leads to a measurement range of 40 kHz to 400 MHz. Within this frequency range the transmission loss is kept lower than 0.5 dB.

B. TOM-X Calibration of VNA

Calibration has a significant impact on the quality of the measurement results. Valid calibration is needed to correct the measured S-parameters at the input port of a VNA. The most important source of measurement uncertainty are unavoidable systematic errors. These include system frequency response, as cable attenuation and phase shift, impedance mismatch or cross coupling within the test setup. The calibration process mathematically derives the systematic error model and corrects the compromised raw data. This error model is an array of vector coefficients used to establish a fixed reference plane of zero phase shift, zero reflection magnitude, lossless transmission magnitude and known system impedance. The array of coefficients is computed by measuring a set of "known" devices or calibration standards connected at a fixed measurement plane [6].

Generally the 12 term error correction model is sufficient, using a calibration kit consisting of a known Short-, Open-, Load- and Through-Standard (SOLT). This method is able to correct all systematic errors of a single channel. As soon as there is cross coupling within the measurement path, e.g. in adaptors, this method cannot correct these errors and measurement data is compromised. For correction of such errors three additional correction coefficients are required, obtaining a 15 term error correction model. Major difference to the SOLT method is a simultaneous measurement of both channel's standards and therefore setup cross coupling can be considered. One 15 term calibration method is the TOM-X method (Through-, Open-, Match-Standard and X-coupling). This process needs a set of four standards, as shown in fig 8. The simultaneous reflection coefficients at both channels are determined with an Open-Open receptacle. The Open-Match jack is used for termination at channel 1 meanwhile reflection on channel 2, and vice versa. The Match-Match standard on both channels and the Through receptacle allow to determine all missing error coefficients [7].

To obtain valid data of the automotive Li-Ion battery, the calibration plane has to be as close as possible to the battery connector. The investigated battery is equipped with an Amphenol ECTA 133 power transmission connector having lead ground coaxial shielding. For a valid calibration on this connector type a calibration kit of identical connector but opposite gender is required (as shown in fig. 8).
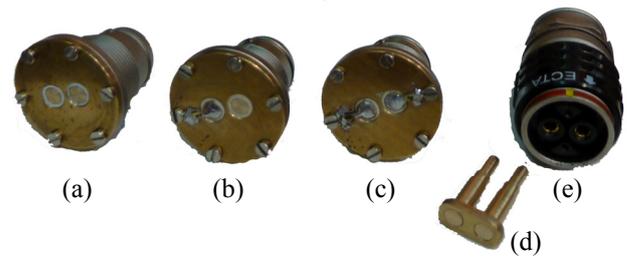
Figure 8   ECTA connector calibration kit for TOM-X calibration, consisting of Open-Open standard (a), Match-Open (b), Match-Match (c), Through (d) and ECTA-SMB coaxial adapter (e).

The cross coupling attenuation within the DC blocking device between channel 1 and channel 2 is beyond 20 dB up to 1 GHz, but the measurement is however compromised by it. Therefore a TOM-X calibration was used and showed superior measurement accuracy compared to the SOLT method.

C. Validation of Calibration Process

In fig. 9 the measured impedance of a $75\,\Omega$ SMD resistor between channel 1 and ground is presented. The blue curve (black in monochrome print) shows its impedance calibrated with the SOLT method, whereas the green (grey) line scopes the measured impedance calibrated with the TOM-X method. Both curves are at a relatively constant value up to 100 MHz, where the TOM-X calibration is more accurate. Above 100 MHz both curves decrease, which is caused by the nonlinearity of the used SMD resistor. Measurements with an Impedance Analyzer show that resistors of this charge reduce their impedance in a comparable way beginning at 100 MHz.
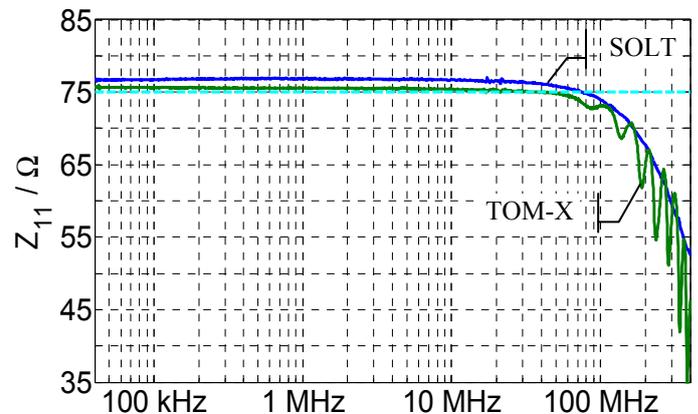
Figure 9   Impedance measurement results of a $75\,\Omega$ SMD resistor with SOLT and TOM-X calibration methods.

Above 100 MHz there is an oscillating behavior of the impedance at the TOM-X calibration, which cannot be seen in the curve of the SOLT calibration. These resonances occur because of impedance mismatches within the DC blocking device and the ECTA-SMB adapter. They do not occur at the SOLT calibration, because there is no DC blocking device inserted, as the SOLT method cannot correct cross coupling. With inserted DC blocking device there could not be achieved valid data of this SMD resistor impedance.

D. Battery Measurement Results

The measured S-parameters of the battery describe its high frequency small-signal behavior and can be transformed into comparable Z-, Y-, H-, or T-parameters [5]. These parameters only describe the battery behavior with special case conditions and cannot be seen as e.g. impedances of a given network. For example the Z-parameters are also called open-circuit impedance parameters as they are determined under open circuit conditions. Z_{11} describes the port 1 input impedance of a two-port and open circuit at port 2 with $Z_{11} = U_1/I_1 |_{I2=0}$, whereas the transmission parameter Z_{12} is calculated as $Z_{12} = U_1/I_2 |_{I1=0}$ with excitation at port 2 and port 1 open circuit voltage. Here the measured S-parameters were converted into Z-parameters.

In fig. 10 and fig. 11 the measured impedance parameters of the investigated Li-Ion battery are illustrated. The blue (grey) curve of fig. 10 shows the reflection impedance Z_{11} and the red (black) one Z_{22}.
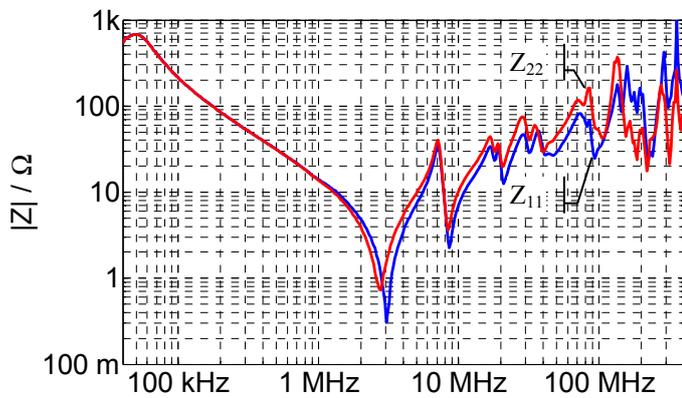
Figure 10   Reflection parameters of an automotive Li-Ion battery.

The transmission impedance parameters Z_{12} are colored in violet (grey), respectively Z_{21} in green (black) and shown in fig 11. The transmission parameters from port 1 to port 2 and vice versa are very similar, and therefore the transmission impedances Z_{12} and Z_{21} in fig. 11 are hardly distinguishable. For most frequencies they have equal values.
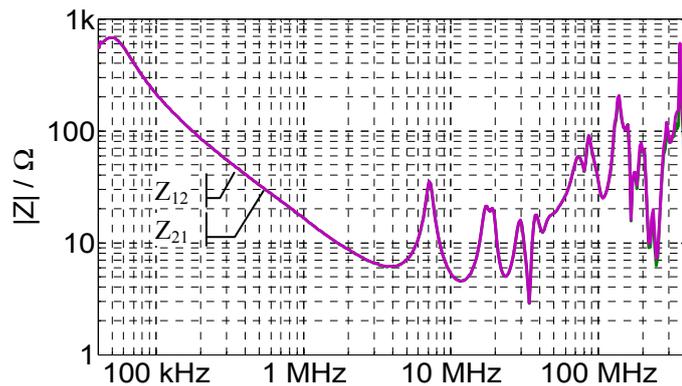
Figure 11   Transmission parameters of an automotive Li-Ion battery.

All four curves show a high-impedance behavior in the low frequency range below 100 kHz, and a decreasing behavior with increasing frequency. The reflection parameters have a series resonance at ~3 MHz and there is a distinct parallel resonance of all four parameters at 7 MHz. Followed by a second series resonance of the reflection parameters at 8.5 MHz there is a increasing behavior of the impedances observable, but no more distinct resonances visible.

V.   CONCLUSION

This paper shows that automotive HV power cables have a characteristic impedance considerably lower than 50 Ω. They show transmission line character in a frequency region of interest for EMC issues. Major termination of these transmission lines for switching devices are HV accumulator batteries. The presented automotive Li-Ion battery shows an impedance behavior from some hundreds of ohms to a few hundred milliohms, from close to open to close to shortened. The battery impedance is transformed by the coaxial transmission lines into a different resonant input impedance of the entire network, which significantly differs to the input impedance of LISNs according to CISPR 25.

This leads to the perception that recently used LV LISNs for EMI testing of HV components imply a mismatch of input impedances. Optimized EMI performance of HV components using LV LISNs may not be reproduced mounted in car and could induce failed vehicle EMC tests. Thus further investigation about EMI testing of HV component conducted emissions is necessary. An AN could be developed, that matches closer the electromagnetic environment of HV components and test results compared to achieve an estimation of EMI performance on vehicle level. Knowledge of high frequency behavior of HV cable and batteries can be used to determine an electronic circuit, representing a minimum HV power network.

VI.   REFERENCES

[1]   Paul, Clayton R.   (1992):   „Introduction   to   Electromagnetic Compatibility", New York: John Wiley & Sons, Inc.

[2]   IEC/CISPR 25:2002 / DIN-EN 55025:2003,   "Radio   disturbance characteristics for the protection of receivers used on board vehicles, boats and on devices – Limits and methods of measurement", European Committee for Electrotechnical Standardization (CENELEC), rue de Stassart 35, B-1050 Bruxelles.

[3]   Yamamoto S., Ozeki, O. "RF Conducted Noise Measurements of Automotive Electrical and Electronic Devices Using Artificial Network", IEEE Trans. Veh. Technol., vol. VT-32, no. 4, pp. 247– 253, Nov. 1983.

[4]   Marko, H. (1971): "Theorie linearer Zweipole, Vierpole und Mehrpole", Stuttgart: S.Hirzel Verlag.

[5]   Jahn S., Margraf M., Habchi V. and Jacob R. (2005): „Qucs – Technical Papers",   qucs.sourceforge.net/docs/technical.pdf,   ch.   1.3   Matrix conversions, pp. 11–16.

[6]   Agilent Technologies (2009): "Application Note 1287-11: Specifying Calibration Standards and Kits for Agilent Vector Network Analyzers", http://cp.literature.agilent.com/litweb/pdf/5989-4840EN.pdf

[7]   Schiek B. (1999): „Grundlagen der Hochfrequenz-Messtechnik", Berlin: Springer-Verlag.